ELSEVIER

Dyes and Pigments 53 (2002) 31–43

DYES and PIGMENTS

www.elsevier.com/locate/dyepig

Thermodynamic and kinetic aspects of self-association of dyes in aqueous solution

Kiyofumi Murakami*

Faculty of Education, Yamaguchi University, Yoshida 1677-1, Yamaguchi 753-8513, Japan

Received 24 July 2001; received in revised form 1 November 2001; accepted 5 December 2001

Abstract

The thermodynamic and kinetic data of monomer–dimer equilibria of dyes and their related substances in aqueous solutions have been reviewed. The enthalpy–entropy compensation relation with the compensation temperature of 273(±5) K was observed. The thermodynamic parameters were found to change with the structure of dye and the species and the concentration of co-existing substances. The kinetic data showed that the compensation relation mainly arose from the forward activation process and there are at least three activation patterns. Redistribution of hydrated water molecules around participating components upon dimerization has been considered to play a central role in these properties. The monomer-dimer equilibria of dyes in aqueous solutions are of great value to be studied as the simplest model systems of many interaction systems. © 2002 Elsevier Science Ltd. All rights reserved.

Keywords: Self-association of dyes; Monomer–dimer equilibria; Thermodynamics; Kinetics; Enthalpy–entropy compensation; Hydration states

1. Introduction

Self-association of dyes and related substances is a very important phenomenon in many fields of applied chemistry such as the dyeing chemistry, biological staining, photographic chemistry, and laser chemistry [1–3]. It is also the most fundamental model reaction of many kinds of molecular interactions such as the micelle formation of amphiphilic substances and the binding of small organic molecules to macromolecules. For example, the co-operative binding phenomena which have frequently been observed in the systems of amphiphiles and linear lattices or proteins, which are closely related to the colloidal and denaturation properties of the macromolecules, originates from the self-association of the bound ligands on the macromolecules [4–7]. For these reasons, a extremely large number of studies have been carried out to reveal the nature of the self-association of dyes. Especially, thermodynamic and kinetic information for the dimerization reaction has been thought to be valuable to clarify the forces acting between interacting molecules and the detailed dimerization mechanism.

In spite of many studies concerning the dimerization equilibria of dyes and related substances, the mechanism seems not to be fully recognized because the experimental conditions such as solvent,

* Tel./fax: +81-83-933-5351.
E-mail address: murakami@edu.yamaguchi-u.ac.jp

0143-7208/02/$ - see front matter © 2002 Elsevier Science Ltd. All rights reserved.
PII: S0143-7208(01)00104-8

coexisting salt and its concentration etc. are different from study to study and many of the discussions have been made referring to the relatively few related studies. Therefore, it is worthwhile to picture the whole feature of the dimerization from the presently-available data and to clarify the subject matter to be explored in the near feature. In this paper, the thermodynamic and kinetic studies on the dimerization equilibria of dyes and related substances have been reviewed to discuss in detail the dimerization mechanism in aqueous solution and the role of the dimerization reaction as the most fundamental model of the other interaction systems.

Table 1
Monomer–dimer equilibria of known thermodynamic parameters

Type	Data number	Ref.
Azo dyes	38	[8(a)–(m)]
Acridine and thiadine dyes	38	[9(a)–(p)]
Xanthene dyes	17	[10(a)–(f)]
Cyanine dyes	7	[11(a)–(e)]
Porphyrins and phthalocyanines	7	[12(a)–(e)]
Anthraquinone dyes	5	[13(a)–(b)]
Benzene and its derivatives	9	[14(a)–(d)]
Purine and pyrimidine derivatives	9	[15(a)–(e)]
Antibiotics	3	[16(a)–(c)]
Alkaloid and its derivatives	6	[17(a)–(b)]
Carboxylic acids	6	[18]

2. Thermodynamic properties

The dimerization equilibrium is expressed by

$$2\mathrm{M} \underset{k_b}{\overset{K_D}{\underset{k_f}{\rightleftarrows}}} \mathrm{D} \quad (1)$$

where M and D are the monomer and dimer forms of dye, respectively, and K_D is the dimerization constant. k_f and k_b are the forward and backward rate constants. The dimerization constant may be expressed by the concentrations of monomer and dimer as

$$K_D = [\mathrm{D}]/[\mathrm{M}]^2 \quad (2)$$

in low reactant concentrations. While a large number of studies evaluated the dimerization constants, a relatively small number of the thermodynamic data such as the standard enthalpy and entropy changes of dimerization (ΔH° and ΔS°) are now available. Table 1 shows the list of these studies [8–18].

2.1. Enthalpy–entropy compensation in monomer–dimer equilibria

The ΔH° vs. ΔS° plot for the dimerization of dyes and related substances in aqueous solution is shown in Fig. 1. This figure shows the tendency that the data of benzene and its derivatives and alkyl carboxylic acids fall on the line which passes near the origin (the broken line), while those of many other dye stuffs having relatively large structures fall on the line being the far side from the origin (the solid line). This difference means that the free energy changes of dimerization for the dye stuffs are smaller than those of the former substances, i.e. the interactions between monomer units for the dyestuffs are stronger than those for the benzene and its derivatives and alkyl carboxylic acids. The linear dependency between ΔH° and ΔS° has been discussed in terms of the enthalpy–entropy compensation relation [19]. The compensation line for the dye systems was calculated by a linear least square-fit analysis as

$$\Delta H^\circ = -21.2(\pm 0.6) \times 10^3 + 273(\pm 5)\Delta S^\circ \quad (3)$$

where the numbers in the parentheses show the standard deviations of the intercept and the slope. The compensation temperature takes the value of $T_c = 273(\pm 5)$ K. The values of ΔH° and ΔS° are distributed over the wide range of magnitude along the compensation line, depending on the structure of the substance and the co-existing salt and so on. The data in the region of $\Delta H^\circ > 0$ and $\Delta S^\circ > 0$ mean the entropy-driven reactions, on the other hand, the data in the region of $\Delta H^\circ < 0$ and $\Delta S^\circ < 0$ mean the enthalpy-driven ones. To understand the factors and the manner in which the position on the compensation line is affected is

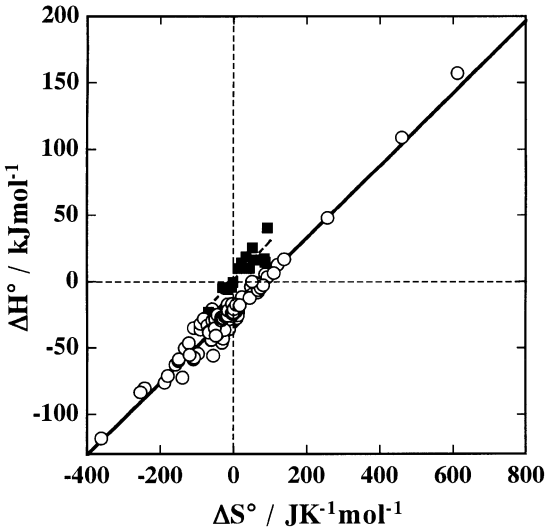

Fig. 1. ΔH° vs. ΔS° plot for the dimerization of dyes and their related substances in aqueous solution. The symbols show the data of dyes (○) and benzene and its derivatives and alkylcarboxylic acids (■). The solid line represents the least square fit to the data of the dye systems [Eq. (3)]. The broken line shows the least square fit to the data for the latter systems.

very important from theoretical and/or applicational view points.

2.2. Effect of structure

In the cases of the benzene and its derivatives and alkyl carboxylic acids, it can be seen that both the values of ΔH° and ΔS° tend to increase from the enthalpy-driven region to the entropy-driven one as the hydrophobicity of the substance increases [14(c),18]. This is the typical behavior of the hydrophobic interaction [20], and may be interpreted by the contribution of the dehydration of hydrophobically-hydrated water molecules on dimerization. For the dye molecule systems, we can also see that the same hydrophobic effect on the thermodynamic parameters is operative, from the data collected for the dye molecules in which different-length alkyl-chains are introduced: alkyl derivatives of Acridine Orange [9(l)], sodium 1-amino-4-alkylaminoanthraquinone-2-sulfonates [13(a)], and oxazolopyridocarbazole [17(b)]. Fig. 2 shows the plots of ΔH° and ΔS° vs. the number of methylene groups of the introduced alkyl chains for these systems as well as that for the above

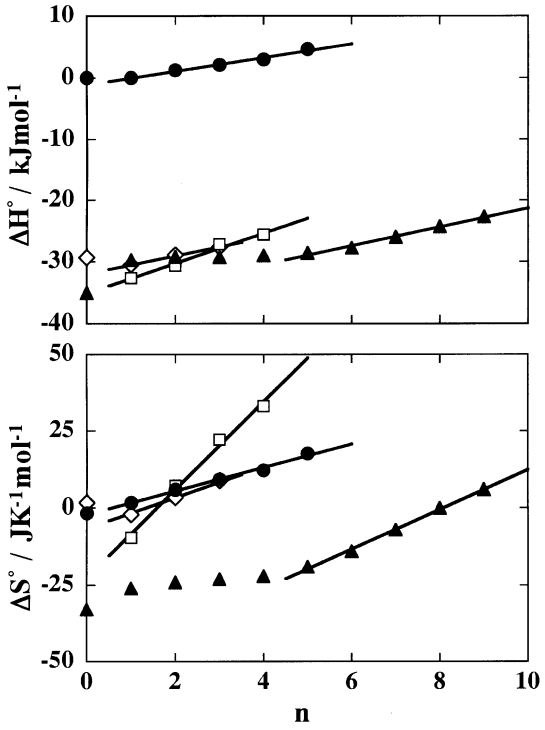

Fig. 2. The plots of ΔH° and ΔS° vs. the number of methylene groups of the introduced alkyl chain for carboxylic acids (●) [18], Acridine Orange (▲) [9(1)], sodium 1,4-aminoanthraquinone-2-sulfonate (□) [13(a)], and oxazolopyridocarbazole (◇) [17(b)]. The solid line for each data shows the least square fit in the region where ΔH° and ΔS° linearly increase with the number of introduced methylene groups.

mentioned alkyl carboxylic acid systems. In the case of the alkyl Acridine Orange, the hydrophobic effect due to the introduced alkyl chain seems to become pronounced for the alkyl chains longer than the butyl group. On the other hand, the hydrophobic effect appears from the shorter alkyl chains for the other systems. This difference may reasonably be interpreted by the difference in dimer configurations, i.e. the anti-parallel orientation for the short-alkyl-chain Acridine Oranges and the parallel orientation for the long-alkyl-chain Acridine Oranges and the other substances [9(l)]. As the average of the slopes of these plots, we can estimate the contribution of the introduced alkyl chain to ΔH° and ΔS° to be 1.6 ($\pm$0.5) kJ and 7.4 ($\pm$4.1) J K^{-1} per mole of methylene group, respectively. Using these values, we can evaluate the contribution of a methylene group to the free energy change of

dimerization as -610 J mol^{-1} at 298 K. This value agrees with the value of -525 J mol^{-1} estimated as the contribution of methylene group to the free energy change due to the interaction between surfactant molecules bound to the protein surface [6].

The values of K_D, ΔH° and ΔS° for the dimerization of halofluorescein dyes have been found to increase with an increase in the sum of atomic polarizability of introduced halogens [10(b)]. The thermodynamic parameters for the dimerization of Acid Red 138, which is in a tautomeric azo-hydrazone equilibrium, have shown the interesting result that the hydrazon form, which has the larger ground-state dipole moment and transition moment than the azo form, takes the larger binding constant and the fairly larger values of ΔH° and ΔS° than those of the azo form, i.e. the differences in ΔH° and ΔS° are 92 kJ mol^{-1} and 337 J K^{-1} mol^{-1}, respectively [8(m)]. If we take account of the dispersion force only between the dye molecules, it could be expected that both the ΔG° and ΔH° decrease with an increase in the polarizability of dye molecule. Contrarily, the observed increases in ΔH° with the polarizability of the dye molecules shows that the redistribution of the hydration water molecules on dimerization serves the predominant contributions to ΔH° and ΔS°. The water molecules strongly hydrated to the monomer molecule by a strong dispersion force may be in the state of a low enthalpy and a low entropy being smaller than those of the bulk water. Dehydration of these water molecules upon dimerization would lead to positive contributions to ΔH° and ΔS°. That is, the larger the polarizability of the dye molecule becomes, the stronger this effect would becomes. As a result, the effect of molecular polarizability on the thermodynamic parameters is similar to the hydrophobic effect in the previous paragraph.

2.3. Effect of salt

There is the well known tendency that the dimerization constant becomes large as the concentration of an added salt increases. This dimer stabilization effect of salt has been explained by the depression of the electrostatic repulsion between charged monomers in the dimer due to the charge-screening effect. Visualization of this effect in more detail is worthwhile to recognize the meaning of the salt effect on the thermodynamic parameters.

The maximum point, at which the surface density of opposite ions in the ionic atmosphere for the 1:1 electrolyte, can be calculated from the Debye–Huckel theory [21] for several ionic strengths as $r_{max} = 68$ nm for $I = 0.00002$, $r_{max} = 9.5$ nm for $I = 0.001$, and $r_{max} = 1.4$ nm for $I = 0.05$. This shows that r_{max} progressively decreases with an increase in ionic strength. That is the screening opposite ions exist in the large space (about 100 times the size of dyes) at the low ionic strength of the order of $I = 10^{-5}$, which is the ordinary experimental condition of salt-free systems, concentrate in the small space comparable to the size of dyes at $I = 0.05$. This means that the hydration state of dye may be highly affected by the presence of the opposite ions at the large-ionic-strength conditions. Since the charge density of the dimer is larger than the monomer, a further uptake of the opposite ions by the dimer would occur as the dimerization takes place. This process may conveniently be expressed by the following stoichiometrical equation.

$$2\mathrm{M} + n\mathrm{OI} \rightleftarrows \mathrm{D}\cdot(\mathrm{OI})_n, \tag{4}$$

where OI means the opposite ion. The equilibrium constant of this reaction may be written as

$$K_0 = \left[\mathrm{D}\cdot(\mathrm{OI})_n\right]/[\mathrm{M}]^2\,[\mathrm{OI}]^n = K_D[\mathrm{OI}]^{-n}, \tag{5}$$

where the number n could not be expected to be an integer. Taking the logarithm of both sides of this equation gives

$$\log K_D = \log K_0 + n \log [\mathrm{OI}]. \tag{6}$$

Using this equation, we can evaluate the amount of the opposite ions being taken up as the slope of log K_D vs. log [OI] plot. The plots for the systems of proflavine and Acridine Orange–KCl [9(f) and (g)], Acid Red 88–NaCl [8(j)], and Biebrich Scarlet–NaCl [8(l)] are shown in Fig. 3. The solid lines are the least square fits. From the slopes of these lines, the numbers of the uptook opposite ions for

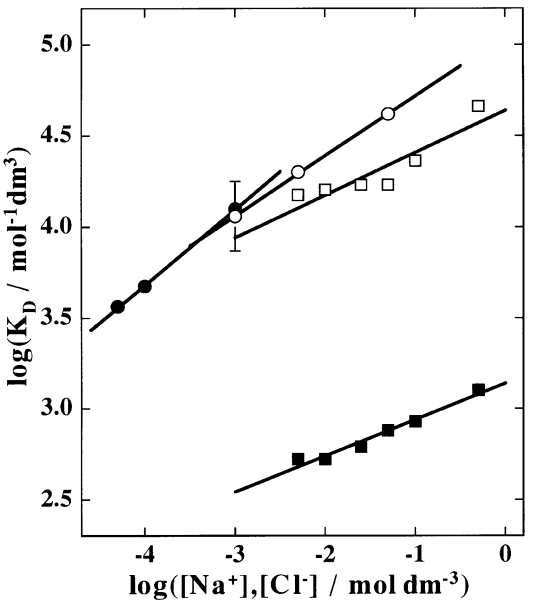

Fig. 3. log K_D vs. log [OI] plots for the systems of Acridine Orange (□), proflavine (■), Biebrich Scarlet (○), and Acid Red 88 (●). The solid lines are the least square fits to the data.

the monocationic dyes were estimated as about 0.2 (0.20 for the proflavine system, and 0.23 for the Acridine Orange system), while those for the azo dyes take larger values as 0.33 (Biebrich Scarlet) and 0.42 (Acid Red 88). The result, that the amount of opposite ions uptook upon dimerization is larger for the azo dyes than those for the acridine dyes, may be due to the fact that the charge for the azo dyes is localized at the sulfonato group but that of the acridine dyes is delocalized.

Concerning the dimerization of Biebrich Scarlet, it was also found that the values of ΔH° and ΔS° poorly depend on the co-existing counter-cation species in the absence of added salt but they spread, depending on the salt-cation species, over the wide range of values along the compensation line in the presence of 0.05 mol dm^{-3} salt [8(l)]. The effect of cation species on the thermodynamic parameters has been classified according to the values of those parameters and the ionic radius (r_{ion}) of the cations, as the first class: Li^+ and Na^+ (small r_{ion} and low ΔH° and ΔS° values), the second class: K^+, Rb^+, Cs^+, and NH_4^+ (intermediate r_{ion} and low ΔH° and ΔS° values), the third class: $(C_2H_5)_4N^+$ and $(C_3H_7)_4N^+$ (large r_{ion} and high ΔH° and ΔS° values), and the forth class: $(CH_3)_4N^+$ (relatively large r_{ion} and low ΔH° and ΔS° values). In each class, the values of ΔH° and ΔS° tend to increase with an increase in ionic radius of cation. Further, this classification showed the interesting agreement with that based on the viscosity B coefficient and the activation energy of viscous flow [22]. These results lead to the conclusion that the thermodynamic parameters of dimerization are highly affected by the hydration structure of the opposite ions being taken up in the dimerization step. The above mentioned behavior has been well interpreted by taking account of the hydrated water structures around cations referred to the bulk water structure, such as the ordered structure around the small cations (the first class), the disordered one around the intermediate-size cations (the second class) and the hydrophobically hydrated structure around the hydrophobic cations (the forth class), and of the two possible events in the dimerization step, that is, the reorientation of water molecules along the electric field formed by the uptake of cation and the dehydration of the hydrated water molecules [8(l)]. In this context, it is noticeable that the decrease of both of the values of ΔH° and ΔS° for the dimerization of Acridine Orange upon KCl addition may be due to the dehydration of the broken-structured water molecules around Cl^- on dimerization [9(o)]. It was also pointed out that the average free energy change for the cooperative binding of Biebrich Scarlet to lysozyme has the value consistent with that for the dimerization in solution [5].

These observations show that both the co-existing salt species and its concentration highly affect the thermodynamic behavior of dye dimerization, depending on their hydration state. We must pay attention to this point to compare the thermodynamic data collected in different salt conditions.

2.4. *Effect of neutral organic substances*

Although many studies have shown that the addition of neutral organic substances such as alcohols and urea generally reduces the dimerization constant, there are few studies concerning the effect on the thermodynamic parameters. The

addition of increasing amount of methanol to the actinomycin-deoxyguanosine binding system successively decreases both of the values of ΔH° and ΔS° of binding [23]. Urea has the similar effect that the addition of increasing amount of urea successively decreases both of the values of the enthalpy and entropy changes of the hydrophobic interaction in the formation of ethane from two methane molecules in aqueous solution [24]. On the other hand, it has been observed that the addition of urea to the anionic azo dye systems (C.I. Acid Red 88 and Acid Red 13) increases both of the values of ΔH° and ΔS° of dimerization [8(g)]. Although no detailed mechanism of the effects has been presented by the authors, it was suggested that the cosolute affects the hydration structure of dye molecules. To recognize the detailed nature of the effects of these substances on dimerization in aqueous systems, many systematical studies are desirable to be explored.

3. Kinetic properties

The number of kinetic data is still fewer than that of the thermodynamic data, but they are very important to realize the dimerization mechanism. From the concentration dependence of the reciprocal relaxation time for the dimerization equilibrium, the rate constants for the forward and backward processes (k_f and k_b) have been evaluated [25]. The activation parameters such as $\Delta H^{\neq}$ and $\Delta S^{\neq}$ have been evaluated using the absolute-reaction-rate theory [26]. In this section, the kinetic data in which activation parameters have been obtained were discussed with much attention as well as the other kinetic data. Table 2 shows the list of these data [27–30].

3.1. Rate constants and activation parameters

Fig. 4 shows the plots of log k_f and log k_b vs. log K_D, which were calculated from the kinetic data measured so far (Table 2). This figure shows that there are two groups of dye, as was pointed out by Inaoka et al. [28(a)]. One is group A, in which the values of the forward rate constant are near the diffusion-controlled limit [31] and the value of log k_b linearly decreases with an increase in log K_D along the line having the slope of -1. The other is group B, in which both the forward and backward rate constants are a few orders of magnitude smaller than those of group A. The difference in the values of the rate constants between these two groups suggests that there are at least two types of activation processes. Among the above kinetic studies, only eight studies for eight substances are

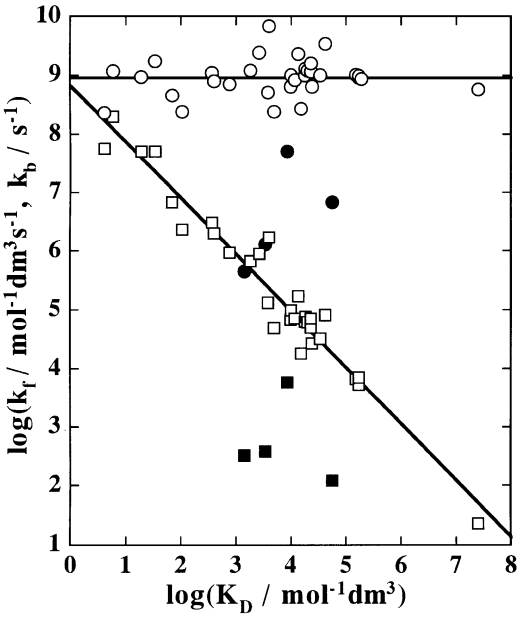

Fig. 4. The plots of log k_f and log k_b vs. log K_D. The circles show the forward rate constants and the squares show the backward ones. The open symbols represent the data for the dyes in group A and the filled symbols represent those in group B (see text).

Table 2
Kinetic data of monomer–dimer equilibria

Type	Data number	Ref
Azo dyes	1	[8(c)]
Acridine and thiadine dyes	20	[9(g),9(i),9(j),9(o)] [27(a)–(i)]
Xanthene dyes	4	[10(d),28(a),28(b)]
Porphyrin dye	1	[29]
Purine and pyrimidine derivatives	3	[15(b),15(e),30]
Antibiotics	1	[16(c)]
Alkaloid and its derivatives	6	[17(b)]

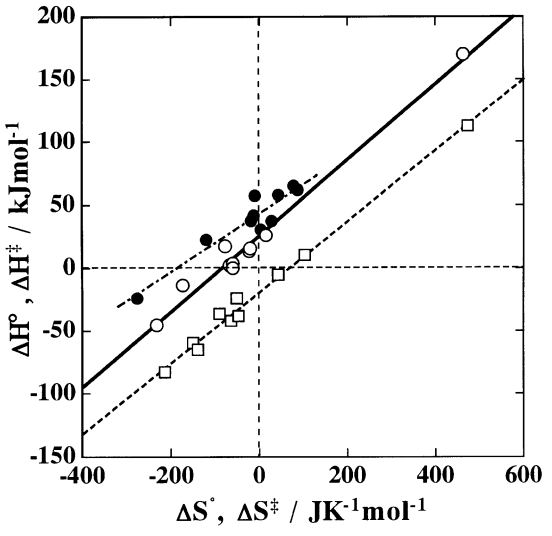

Fig. 5. ΔH° vs. $\Delta S^{\neq}$ plots for the forward process (○) and the backward one (●) for the dimerization reaction. Some of these data were calculated by this author from the literature values for the temperature dependence of the rate constants. The ΔH° vs. ΔS° plot (□) is also shown for comparison. The straight lines are the least square fits to these data sets.

concerned with the temperature dependence of the rate constants [8(c),9(i),9(j),9(o),10(d),15(b),15(e), 27(b)], from which the detailed nature of the activation processes may be examined. Fig. 5 shows the plot of $\Delta H^{\neq}$ vs. $\Delta S^{\neq}$ values for the forward and backward processes of the dimerization as well as the ΔH° vs. ΔS° plot. We can see from this figure that the enthalpy–entropy compensation relation observed for the equilibrium thermodynamic parameters [Fig. 1 and Eq. (3)] results mainly from the forward activation process.

Fig. 6 shows the activation-energy profiles, in which the activation-volume profile for Methylene Blue [27(h)] is also shown. In this figure, the dyes are arranged in the order of the entropy pattern. The following points may be noteworthy. (1) The dimerizations of proflavine, Acridine Orange, Methylene Blue, and *N*,*N*-dimethyladenosine, which all belong to group A in Fig. 4, are the enthalpically-driven reactions, on the other hand, those of Congo Red, Rhodamine B and Rhodamine 3B (group B in Fig. 4) are entropically driven. The structural feature common for the three dyes

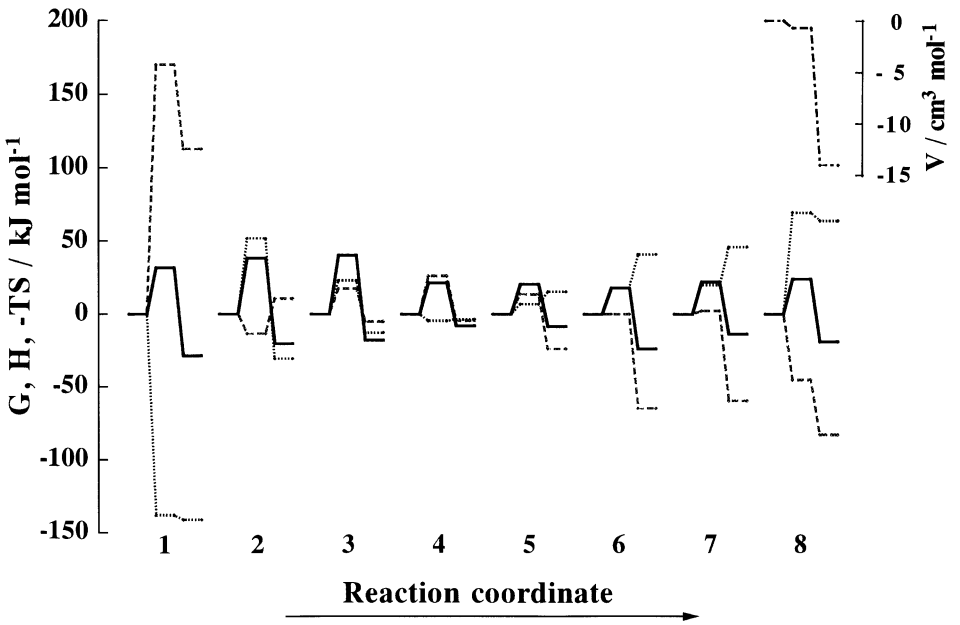

Fig. 6. Activation energy profiles for the dimerization of dyes and related substances; 1: Congo Red, 2: Rhodamine 3B, 3: Rhodamine B, 4: *N*,*N*-dimethyladenine, 5: *N*,*N*-dimethyladenosine, 6: Acridine Orange, 7: proflavine, and 8: Methylene Blue. The lines shows the free energy profile (solid line), the enthalpy profile (dashed line), and the entropy profile which is expressed by multiplying-*T* (dotted line). The volume profile is also depicted for Methylene Blue.

(proflavine, Acridine Orange, and Methylene Blue) in group A is that they have similar backbone ring structures (acridine or phenothiazine), and that for the latter three dyes in group B is that they have relatively large hydrophobic groups (two naphthalene rings and two benzene rings for Congo Red, and four and five ethyl groups for Rhodamine B and Rhodamine 3B, respectively). (2) The activation enthalpy of the forward process has positive values for Congo Red, Rhodamine B, *N*,*N*-dimethyladenine, and *N*,*N*-dimethyladenosine, nearly zero for proflavine and Acridine Orange, and negative values for Rhodamine 3B and Methylene Blue. On the other hand, the activation enthalpy of the reverse process has positive values for all the dyes except Rhodamine 3B. In any case, the positive activation-enthalpy means that some net bonds are broken in the activation process. The negative activation enthalpy has been interpreted by considering the combination of two substeps, i.e. the diffusion-controlled association of two monomers and the transformation of the complex into the dimer (see the next section) [9(j)]. (3) The values of the activation entropy of the forward process are negative or nearly zero for all the dyes except Congo Red (this does hold even if considering the unitary entropy [32]), showing that the structures of the activated states of those dyes are reduced in freedom compared to the monomer states. The large positive activation entropy in the forward process for Congo Red might be due to the dehydration of the hydrophobically-hydrated water molecules, since it is difficult to consider that the freedom of the structure of the dye molecule itself increases in the approach of monomer molecules. Along the same line, the entropy increases in the process from the activated state to the stable dimer for Rhodamine B and Rhodamine 3B might be ascribed to the dehydration of the hydrophobically-hydrated water molecules around the alkyl groups. That is the dyes in group B may be divided into two subgroups depending on the process in which the entropy value increases. In summary, there are at least three patterns in the activation energy profile, according to the structure of the dye. (4) The activation volume profile for Methylene Blue suggests that the ejection of hydrated water molecules takes place in the process from the activated state to the stable dimer.

3.2. Detailed mechanism

In order to consider the reaction mechanism in further detail, it is convenient to divide Eq. (1) into two substeps as

$$2\mathrm{M} \underset{k_{-1}}{\overset{k_1}{\rightleftarrows}} \mathrm{M} \bullet \mathrm{M} \underset{k_{-2}}{\overset{k_2}{\rightleftarrows}} \mathrm{D} \tag{7}$$

where, the first step is the diffusion-controlled encounter-complex formation, and the second step is the stable-dimer formation. k_1, k_{-1}, k_2, and k_{-2} are the rate constants of each process. Under the steady state approximation for the encounter complex, Eq. (7) gives a single relaxation, and the forward and backward rate constants are given by

$$k_\mathrm{f} = \frac{k_1 k_2}{k_{-1} + k_2} \tag{8}$$

$$k_\mathrm{b} = \frac{k_{-1} k_{-2}}{k_{-1} + k_2} \tag{9}$$

The following two extreme cases are valuable to be considered. In the case of $k_{-1} \ll k_2$, Eqs. (8) and (9) become

$$k_\mathrm{f} = k_1 \tag{10}$$

$$k_\mathrm{b} = \frac{k_{-1}}{K_2} \tag{11}$$

That is, the forward rate constant agrees with that of the diffusion-controlled association, and the backward rate constant is that of the diffusion-controlled dissociation divided by K_2. The rate constant of the diffusion-controlled association has theoretically been estimated as about 3×10^9 $\mathrm{s}^{-1}\ \mathrm{mol}^{-1}$ [31(c)]. Many of the dyes in group A in Fig. 4, for which the values of the forward rate constant are close to this value, seem to be in this case. On the other hand, in the case of $k_{-1} \gg k_2$, Eqs. (8) and (9) become

$$k_\mathrm{f} = K_1 k_2 \tag{12}$$

$$k_b = k_{-2}. \quad (13)$$

This means that there exists an rapid diffusional pre-equilibrium before the stable dimer formation. Since the value of K_1 is ordinarily in the order of 1 mol^{-1} dm^3, k_f can take an extremely small value compared to that of the diffusion-controlled reaction, depending on the k_2 value. This situation may hold for all of the dyes in group B, and for some dyes in group A in Fig. 4, having relatively small k_f values. The origin of the negative activation enthalpy for the forward process of Methylene Blue dimerization has been attributed to the dipole–dipole and/or ion–dipole interactions in the diffusion-controlled step [9(j)].

3.3. Solvent effect on rate constants

The effect of the addition of alcohols, urea, and glycerol on the rate constants of dimerization of Thionine and proflavine in aqueous solutions [27(e) and (f)] and that of ethyleneglycol on deuterohemin dimerization [29] have been studied. In both cases, it was found that the values of k_f decrease while those of k_b increase on an addition of the additives. The origin of this behavior has been interpreted in terms of the specific and preferential binding of these additives to the dyes by the dispersion forces [27(f)].

4. Comparison with other interaction systems

Fig. 7 shows the few examples of the ΔH° vs. ΔS° plot for the complex formation between alkyl derivatives of dyes and poly(vinylpyrrolidone) [33], DNA [34], and serum albumin [35], and for the dimerization of actins [36], as well as the compensation line of this paper [Eq. (3): solid line] and that reported for drug-receptor bindings (dashed line) [37]. In these cases, the values of ΔH° and ΔS° increase with an increase in the hydrophobicity of dye or actin, in parallel with the compensation lines. This behavior may be the result of the redistribution of the hydrated water molecules around the ligand's hydrophobic groups and the actin's binding sites. It was also found that the hydrophobic side chains of oligo peptides have

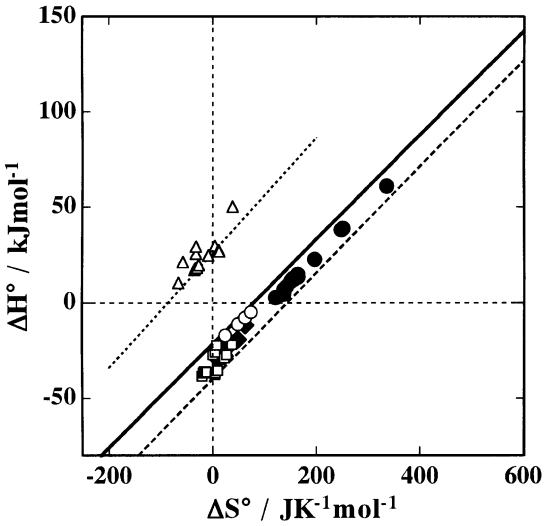

Fig. 7. The comparison of ΔH° vs. ΔS° plots for complex formations between alkyl derivatives of dyes and macromolecules and for a protein dimerization with the compensation line for the monomer–dimer equilibria of dyes (solid line, Eq. 3) and that for the drug–receptor bindings (dashed line) [37]. (○): 4-[4-(dialkylamino)phenylazo]benzenesulfonates–poly(vinylpyrrolidone) systems [33], (□): alkyl Acridine Orange–DNA systems [34], (◆): dancyl amino acids–bovine serum albumin systems [35], and (●): actin dimerization systems [36]. The plot of $\Delta H^{\neq}$ vs. ΔS for the association process of antibody–hapten binding [39] is also shown(☆), being compared with the line (dotted line) for the forward activation process of the dye dimerization.

positive contribution to ΔH° and ΔS° for their binding to neurophysins [38]. The authors of ref.37 have ascribed the origin of the compensation relation to the redistribution of the hydrogen bonds between water, drug and binding site on the binding event [37]. Their interpretation is very attractive. However, the present paper has shown that the enthalpy–entropy compensation relation may come from several kinds of interactions in water. The nature of hydration, including hydrophobic hydration, of the reactants seems to play the key role. It is, therefore, desirable to extend the idea of them so as to involve the redistribution of many kinds of hydrated water molecules around interacting constituents, instead of limiting to the hydrogen bonds. In the case of the actin dimerization, it was shown that the order of the values of the thermodynamic parameters agrees with the order of the body temperature of the species [36].

As was pointed out by the authors, this fact suggests that the hydrophobic nature of actin and the resultant thermodynamic behavior of its self-assembly are closely related to its biological role, i.e. the maintenance of the critical monomer concentration at the low level under physiological conditions. The plot of $\Delta H_f^{\neq}$ vs. $\Delta S_f^{\neq}$ for the antibody-hapten bindings [39], which is also depicted in Fig. 7, shows that these data fall on the line for the forward activation process of dye dimerization. All these examples show that the thermodynamic and kinetic properties of dye dimerization would give us useful insights into the interaction mechanism of many other interaction systems.

5. Concluding remarks

The thermodynamic and kinetic data for the dimerization of dyes in aqueous solutions revealed the enthalpy–entropy compensation relation and its relation to the activation processes. The hydration structures of the constituents and their changes upon dimerization play the central role in this phenomenon. The similarity of the thermodynamic and kinetic behavior of the dye dimerization to that of the other interaction systems shows the significance of the dimerization reaction as the simplest model system. Further systematical studies to clarify the mutual relation between dye structures, hydration states, and the thermodynamic and kinetic properties are now desired to be explored.

References

[1] Zollinger H. Color chemistry: syntheses, properties and applications of organic dyes and pigments. New York: VCH, 1991. .

[2] Wyn-Jones E, Gormally J, editors, Aggregation processes in solutions. Amsterdam: Elsevier, 1983.

[3] Duff D.G., Giles C. In: Franks F., editors, Water: comprehensive treatise, vol. 4. New York: Plenum Press, 1975 [chapter 3]

[4] Murakami K. Cooperative ligand binding to globular protein (I). Bull Chem Soc Jpn 1998;71:2293–8.

[5] Murakami K, Tsurufuji K. Cooperative ligand binding to globular protein (II). Bull Chem Soc Jpn 1999;72:653–9.

[6] Murakami K. Cooperative ligand binding to globular protein: a statistical mechanical theory based on a simple geometrical model and its application to lysozyme systems. Langmuir 1999;15:4270–5.

[7] Moriyama Y, Takeda K, Murakami K. Electrophoretic behavior of complexes between sodium dextran sulfate and cationic surfactants. Langmuir 2000;16:7629–33.

[8] (a) Coates E, Rigg B. Complex formation: relevant data for Solochrome Violet R. Trans Faraday Soc 1961; **57**:1637–45.
(b) Monahan AR, Blossey DF. The aggregation of arylazonaphthols. I J Phys Chem 1970;74: 4014–21.
(c) Yasunaga T, Nishikawa S. Kinetic studies of association and dissociation reactions of Congo Red by the temperature-jump method. Bull Chem Soc Jpn 1972, **45**: 1262–63.
(d) Styanov ST, Deligeorgiev T, Simov D. Spectrophotometric investigation on the aggregation in water of some benzothiazole cationic dyes. J Mol Struct 1984;115:363–66.
(e) Skrabal P, Bangerter F, Hamada K, Iijima T. Entropy contribution to an azo dye aggregation in aqueous solution. Dyes and Pigments 1987;8:371–74.
(f) Hamada K, Fujita M, Mitsuishi M. Aggregation behavior of an azo dye containing a trifluoromethyl group on poly(vinylpyrrolidone). J Chem Soc Faraday Trans 1990;86:4031–35.
(g) Hamada K, Nonogaki H, Fukushima Y, Munkhbat B, Mitsuishi M. Effects of hydrating water molecules on the aggregation behavior of azo dyes in aqueous solutions. Dyes and Pigments 1991;16:111–18.
(h) El-Fass MM, Sallam HB, El-Sabbagh LA, Mahmoud AA. Comparative study of self association of C.I. Reactive Orange 13 in aqueous medium. Polish J Chem 1993;67: 285–92.
(i) Hamada K, Mituishi M, Ohira M, Miyazaki K. Positional effects of a trifluoromethyl group on the aggregation of azo dyes in aqueous solutions. J Phys Chem 1993;97:4926–29.
(j) Simoncic B, Span J, Vesnaver G. A study of the self-association of simple azo dyes using the potentiometric method. Dyes and Pigments 1994;26:257–276.
(k) Hamada K, Yamada K, Mitsuishi M, Ohira M, Mesuda K. Thermodynamic study of the aggregation of azo dyes containing two trifluoromethyl groups in aqueous solutions. J Chem Soc Faraday Trans 1995;91:1601–05.
(l) Murakami K, Kimura Y, Saito M. Thermodynamic study of the effects of monovalent cations on dimerization of a dianionic azo dye, 2-[(2-hydroxy-1-naphthyl)azo]-5[(4-sulfonatophenyl)azo]benzenesulfonate, in aqueous salt solutions. Bull Chem Soc Jpn 1997;70:115–21.
(m) Iijima T, Jojima E, Antonov L, Styanov ST, Styanova T. Aggregation and tautomeric properties of CI Acid Red 138. Dyes and Pigments 1998;37:81–92.

[9] (a) Rabinowitch E, Epstein LF. Polymerization of dyestuffs in solution. thionine and Methylene Blue. J Am Chem Soc 1941;63:69–78.

(b) Zanker V. The proof of definite reversible association of acridine orange by absorption and fluorescence measurements in aqueous solution. Z Physik Chem 1952;199:225–58.
(c) Haugen GR, Melhuish WH. Association and self-quenching of proflavine in water. Trans Faraday Soc 1964;60:386–94.
(d) Shiano DDF, Sturtevant JM. Calorimetric investigations of the binding of inhibitors to α-chymotrypsin I. Biochemistry 1969;8:4910–17.
(e) Mukerjee P, Ghosh AK. Thermodynamic aspects of the self-association and hydrophobic bonding of Methylene Blue. J Am Chem Soc 1970;92:6419–24.
(f) Schwarz G, Klose S, Balthasar W. Cooperative binding to linear biopolymers 2. Thermodynamic analysis of the proflavine–poly(L-glutamic acid) system. Eur J Biochem 1970;12:454–60.
(g) Schwarz G, Balthasar W. Cooperative binding to linear biopolymers 3. Thermodynamic and kinetic analysis of the Acridine Orange–poly(L-glutamic acid) system. Eur J Biochem 1970;12:461–7.
(h) Robinson BH, Loffler A, Schwarz G. Thermodynamic behavior of Acridine Orange in solution. J Chem Soc Faraday Trans 1 1973;69:56–69.
(i) Robinson BH, Loffler A, Schwarz G. Kinetic and amplitude measurements for the process of association of Acridine Orange studied by temperature-jump relaxation spectroscopy. J Chem Soc Faraday Trans 1 1975;71:815–30.
(j) Spencer W, Sutter JR. Kinetic study of the monomer–dimer equilibrium of Methylene Blue in aqueous solution. J Phys Chem 1979;83:1573–6.
(k) Constantino L, Ortona O, Sartorio R, Silvestri L, Vitagliano V. Association equilibria of some 10-n-alkyl 3,6-bisdimethylamino acridinium salts in aqueous solution. Adv Mol Relax Interact Proc 1981;20:191–8.
(l) Septinus M, Seiffert W, Zimmermann HW. Hydrophobic acridine dyes for fluorescence staining of mitochondria in living cells 1. Histochemistry 1983; 79:443–56.
(m) Constantino L, Guarino G, Ortona O, Vitagllano V. Acridine Orange association equilibrium in aqueous solution. J Chem Eng Data 1984;29:62–6.
(n) Braswell EH. Sedimentation and absorption spectroscopy studies of some self-associating cationic dyes. J Phys Chem 1984;88:3653–8.
(o) Murakami K, Mizuguchi K, Kubota Y, Fujisaki Y. Equilibrium and kinetic studies of the dimerization of Acridine Orange and its 10-alkyl derivatives. Bull Chem Soc Jpn 1986;59:3393–7.
(p) Templeton DM. General occurrence of isosbestic points in the methachromatic dye complexes of sulphated glycosaminoglycans. Int J Biol Macromol 1988;10:131–6.

[10] (a) Rohatgi KK, Singhal GS. Nature of bonding in dye aggregates. J Phys Chem 1966;70:1695–701.
(b) Rohatgi KK, Mukhopadhyay AK. Aggregation properties of anions of fluorescein and halofluorescein. J Indian Chem Soc 1972;49:1311–20.
(c) Selwyn JE, Steinfeld JI. Aggregation equilibria of xanthene dyes. J Phys Chem 1972;76:762–74.
(d) Wong MM, Schelly ZA. Solvent-jump relaxation kinetics of the association of rhodamine type laser dyes. J Phys Chem 1974;78:1891–5.
(e) Arbeloa L. Dimeric and trimeric states of the fluorescein dianion. J Chem Soc Faraday Trans 2 1981;77:1725–33.
(f) Arbeloa FL, Gonzalez IL, Ojeda PR, Arberoa IL. Aggregate formation of Rhodamine 6G in aqueous solution. J Chem Soc Faraday Trans 2 1982;78:989–94.

[11] (a) Padday JF. Metachromasy of a thiacarbocyanine dye in aqueous solution: the formation of dimers and trimers. J Phys Chem 1968;72:1259–64.
(b) Matsubara T, Tanaka T. Dissociation equilibrium of dimeric associates of an anionic oxacarbocyanine dye. J Soc Photogr Sci Technol Jpn 1989;52:395–9.
(c) Matsubara T, Tanaka T. Dimerization and j-aggregation thermodynamics of an anionic oxacarbocyanine dye in solution. J Imaging Sci 1991;35:274–8.
(d) Zhang Z, Hao J, Wu B, Yuan H. Thermodynamics of a blue-sensitizing cyanine dye in aqueous methanol solution. J Imaging Sci Technol 1995;39:373–4.
(e) Zakharova GV, Chibisov AK. Spectral investigation of the monomer–dimer equilibrium for thiacarbocyanine dyes. High Energ Chem 1998;32:403–6.

[12] (a) White WJ, Plane RA. A homologous series of water-soluble porphyrins and metalloporphyrins: synthesis, dimerization, protonation and self-complexation. Bioinorg Chem 1974;4:21–35.
(b) Karns GA, Gallagher WA, Elliot WB. Dimerization constants of water-soluble porphyrins in aqueous alkali. Bioorg Chem 1979;8:69–81.
(c) Margalit R, Rotenberg M. Thermodynamics of porphyrin dimerization in aqueous solutions. Biochem J 1984;219:445–50.
(d) Yang YC, Ward JR, Seiders RP. Dimerization of cobalt(II) tetrasulfonated phthalocyanine in water and aqueous alcoholic solutions. Inorg Chem 1985;24: 1765–9.
(e) Cohen S, Margalit R. Physicochemical studies of processes involving potential photodynamic drugs on route to their target: self-aggregation and membrane-binding of Zn-hematoporphyrin. Arch Biochem Biophys 1986;247: 57–61.

[13] (a) Sivarajaiyer SR, Singh GS. Aggregation of anionic dyes in aqueous solutions. J S D C 1973;89:128–32.
(b) Gilkerson WR, Mixon AL. The association of aromatic anions in water. J Sol Chem 1990;19:491–505.

[14] (a) Tucker EE, Lane EH, Christian SD. Vapor pressure studies of hydrophobic interactions. Formation of benzene–benzene and cyclohexane–cyclohexanol dimers in dilute aqueous solution. J Sol Chem 1981;10:1–20.
(b) Bernal P, Christian SD, Tucker EE. Vapor pressure studies of hydrophobic association. Thermodynamics of fluorobenzene in dilute aqueous solution. J Sol Chem 1986;15:947–56.

(c) Strong LE, Brummel CL, Ryther R, Radford JR, Pethybridge AD. Dimerization of some substituted benzoic acids in aqueous solution from conductance measurements. J Sol Chem 1988;17:1145–67.

[15] (a) Gill SJ, Downing M, Sheats GF. The enthalpy of self-association of purine derivatives in water. Biochemistry 1967;6:272–6.
(b) Porschke D, Eggers F. Thermodynamics and kinetics of base-stacking interactions. Eur J Biochem 1972;26;490–498.
(c) Marenchic MG, Sturtevant JM. Calorimetric investigation of the association of various purine bases in aqueous media. J Phys Chem 1973;77:544–8.
(d) Bertz R, Lustig A, Schwarz G. Self-association studies of two adenine derivatives by equilibrium ultracentrifugation. Biophys Chem 1974;1:237–41.
(e) Heyn MP Nicola CV, Schwarz G. Kinetics of the base-stacking reaction of N6,N6-dimethyladenosine. An ultrasonic absorption and dispersion study. J Phys Chem 1977;81:1611–7.

[16] (a) Crothers DM, Sabol SL, Ratner DI, Muller W. Studies concerning the behavior of actinomycin in solution. Biochemistry 1968;7: 1817–23.
(b) Chaires JB, Dattagupta N, Crothers DM. Self-association of daunomycin. Biochemistry 1982;21:3927–32.
(c) Oncescu T, Iliescu I, De Mayer L. Self-association of violamycin (VBI). Biophys Chem 1993;47:277–83.

[17] (a) Engelborghs Y. A thermodynamic study of colchicine and colcemid dimerization. J Biol Chem 1981;256:3276–8.
(b) Adenier A, Aubard J, Schwaller MA. Thermodynamics and kinetics of aggregation processes in aqueous media of ellipticine derivatives: the alkyl-oxazolopyridocarbazole series. J Phys Chem 1992;96:8785–91.

[18] Yamamoto K, Nishi N. Hydrophobic hydration and hydrophobic interaction of carboxylic acids in aqueous solution: mass spectrometric analysis of liquid fragments isolated as clusters. J Am Chem Soc 1990;112:549–58.

[19] (a) Leffler JE, Grunwald E. Rates and equilibria of organic reactions. New York: Wiley, 1963.
(b) Lumry R, Rajender S. Enthalpy–entropy compensation phenomena in water solutions of proteins and small molecules: a ubiquitous property of water. Bioplolymers 1970;9:1125–7.
(c) Exner O. Enthalpy–entropy relation. Progr Phys Org Chem 1973;10:411–82.
(d) Linert W, Han LF, Lukovits I. The use of isokinetic relationship and molecular mechanics to investigate molecular interactions in inclusion complexes of cyclodextrins. Chem. Phys 1989;139:441–82.
(e) Grunwald E, Steel C. Solvent reorganization and thermodynamic enthalpy–entropy compensation. J Am Chem Soc 1995;117:5687–92.

[20] (a) Frank HS, Evans MW. Free volume and entropy in condensed systems III. Entropy in binary liquid mixtures; partial molal entropy in dilute solutions; structure and thermodynamics in aqueous electrolytes. J Chem Phys 1945;13:507–32.
(b) Kauzmann W. Some factors in the interpretation of protein denaturation. Adv Protein Chem 1959;14:1–63.
(c) Nemethy G, Scheraga HA. Structure of water and hydrophobic bonding in proteins. J Chem Phys 1962;36:3382–417.
(d) Tanford C. The hydrophobic effect—formation of micelles and biological membranes. New York: Wiley, 1973.
(e) Ben-Naim A. Hydrophobic interactions. New York: Plenum Press, 1980.
(f) Israelachvili JN, Intermolecular and surface forces. 2nd ed. New York: Academic Press, 1991.

[21] (a) Debye P, Huckel E. The theory of electrolytes. I. Lowering of freezing point and related phenomena. Phys Z 1923;24:185–206.
(b) Robinson RA, Stokes RH. Electrolyte solutions. 2nd ed. London: Butterworths, 1959.

[22] Nightingale ER. In: Conway BE, Barrada RG, editors. Chemical physics of ionic solutions. New York: Wiley, 1966. p. 87–100.

[23] Crothers DM, Ratner DI, Thermodynamic studies of a model system for hydrophobic bonding. Biochemistry 1968;7:1823–7.

[24] Ben-Naim A, Yaacobi M. Effects of solutes on the strength of hydrophobic interaction and its temperature dependence. J Phys Chem 1974;78:170–5.

[25] Bernasconi CF. Relaxation kinetics. New York: Academic Press, 1976. p. 15.

[26] (a) Wynne-jones WFK, Eyring H. Absolute rate of reactions in condensed phases. J Chem Phys 1935;3:492–502.
(b) Glasstone S, Laidler KJ, Eyring H. The theory of rate processes. New York: McGraw-Hill, 1941

[27] (a) Hammes GG, Hubbard CD. The interaction of Acridine Orange with poly-α-L-glutamic acid. J Phys Chem 1966;70:1615–22.
(b) Turner DH, Flynn GW, Lundberg SK. Dimerization of proflavine by the laser Raman temperature-jump method. Nature 1972;239:215–17.
(c) Turner DH, Yuan R, Flynn GW, Sutin N. Kinetics of the stacking of Ethidium Bromide by the Raman laser temperature-jump method. Biophys Chem 1974;2:385–9.
(d) Inaoka W, Harada S, Yasunaga T. Kinetic studies of the dimerization reaction of thionine by the laser temperature-jump method. Bull Chem Soc Jpn 1978;51: 1701–3.
(e) Dewey TG, Wilson PS, Turner DH. Solvent effects on stacking. A kinetic and spectroscopic study of thionine association in aqueous alcohol solutions. J Am Chem Soc 1978;100:4550–4.
(f) Dewey TG, Raymond D, Turner DH. Laser temperature jump study of solvent effects on proflavine stacking. J Am Chem Soc 1979;101:5822–6.
(g) Gormally J, Natarajan N, Wyn-Jones E, Attwood D, Gibson J, Hall DG. Aggregation by stacking of a drug in aqueous solution studied by means of light scattering and ultrasonic relaxation. J Chem Soc Faraday Trans 2 1984;80:243–59.

(h) Ohling W. The effect of pressure on the self-association of dyes in aqueous solutions studied by cable temperature-jump relaxation spectroscopy. Ber Bunsenges Phys Chem 1984;88:109–15.
(i) Adenier A, Aubard J. Determination par spectrophotometrie d'absorption differentielle et relaxation chimique par saut de temperature des parametres caracterisant l'autoassociation de colorants en solution aqueuse (1). J Chim Phys 1987;84:921–7.

[28] (a) Inaoka W, Harada S, Yasunaga T. Kinetic and spectrophotometric studies of Rhodamine 6G dimerization in aqueous solution. Bull Chem Soc Jpn 1980;53:2120–2.
(b) Inaoka W, Harada S, Fujii S, Yasunaga T. Dimerization kinetics of fluoresceine in aqueous solution. Bull Chem Soc Jpn 1982;55:607–8.

[29] Gushimana Y, Doepner B, Hackert EM, Ilgenfritz G. Kinetics of quinine–deuterohemin binding. Biophys Chem 1993;47:153–62.

[30] Garland F, Christian SD. Thermodynamic and kinetic model of sequential nucleoside base aggregation in aqueous solution. J Phys Chem 1975;79:1247–52.

[31] (a) Smoluchowski MV. Drei vortrage uber diffusion, brownsche molekularbewegung und koagulation von kolloidteilchen. Z Phys 1916;17:557–71, 585–99.
(b) Smoluchowski MV. Versuch einer methematischen theorie der koagulationskinetik kolloider losungen. Z Phys Chem 1917;92:129–68.
(c) Eigen M. Kinetics of high-speed ion reactions in aqueous solution. Z Phys Chem NF 1954;1:176–200.

[32] Gurney RW. Ionic processes in solution. New York: McGraw-Hill, 1953 [chapter 6]

[33] Takagishi T, Kuroki N. Interaction of polyvinylpyrrolidone with Methyl Orange and its homologs in aqueous solution: thermodynamics of the binding equilibria and their temperature dependencies. J Polym Sci 1973;11:1889–901.

[34] Kubota Y, Eguchi Y, Hashimoto K, Wakita M, Honda Y, Fujisaki Y. Equilibrium dialysis studies of the DNA–acridine complexes. Bull Chem Soc Jpn 1976;49:2424–6.

[35] Seki T, Komiyama J, Iijima T, Wild P. The interaction of dansyl amino acids with bovine serum albumin. Colloid Polym Sci 1984;262:311–8.

[36] Swezey RR, Somero GM. Polymerization thermodynamics and structural stabilities of skeletal muscle actins from vertebrates adapted to different temperatures and hydrostatic pressures. Biochemistry 1982;21:4496–503.

[37] Gilli P, Ferretti V, Gilli G, Borea PA. Enthalpy–entropy compensation in drug–receptor binding. J Phys Chem 1994;98:1515–18.

[38] Whittaker BA, Allewell NM, Carison J, Breslow E. Enthalpy of ligand binding to bovine neurophysins. Biochemistry 1985;24:2782–90.

[39] Pecht I, Lancet D. In: Pecht I, Rigler R, editors Chemical relaxation in molecular biology. New York: Springer-Verlag; 1977. p. 306–38.